POLITECNICO DI TORINO
Repository ISTITUZIONALE

Vibration and buckling of open TWBs with local weakening

Original
Vibration and buckling of open TWBs with local weakening / Piana, G., Carpinteri, A., Lofrano, E., Ruta, G.. - In: PROCEDIA ENGINEERING. - ISSN 1877-7058. - ELETTRONICO. - 199:(2017), pp. 242-247. (X International Conference on Structural Dynamics, EURODYN 2017 Rome 10-13 September, 2017) [10.1016/j.proeng.2017.09.012].

Availability:
This version is available at: 11583/2689719 since: 2021-07-19T15:15:06Z

Publisher:
Elsevier

Published
DOI:10.1016/j.proeng.2017.09.012

Terms of use:

This article is made available under terms and conditions as specified in the corresponding bibliographic description in the repository

Publisher copyright

(Article begins on next page)

07 November 2026

Available online at www.sciencedirect.com

ScienceDirect

Procedia Engineering 199 (2017) 242–247

Procedia Engineering

www.elsevier.com/locate/procedia

X International Conference on Structural Dynamics, EURODYN 2017

Vibration and buckling of open TWBs with local weakening

G. Piana[a,b,*], A. Carpinteri[b], E. Lofrano[a], G. Ruta[a]

[a]*Department of Structural and Geotechnical Engineering, University "La Sapienza", via Eudossiana 18, 00184 Rome, Italy*
[b]*Department of Structural, Geotechnical and Building Engineering, Politecnico di Torino, corso Duca degli Abruzzi 24, 10129 Turin, Italy*

Abstract

Free vibration and Ljapounov stability of compressed open thin-walled beams with a cross-section reduction are studied by a *in-house* finite differences numerical code, based on a refined direct beam model and allowing for investigating elastic stability of non-trivial equilibrium paths in a dynamic setting. The benchmark is a beam with doubly symmetric cross-section and non-zero warping rigidity, under free, semi-, and fully restrained warping at its ends. In all cases, the results of the direct model are compared to finite element and/or experimental ones. The reduction in the cross-section rigidity induces a weakening that may model a local damage; thus, the present investigation may be useful with an outlook to damage monitoring and identification.

© 2017 The Authors. Published by Elsevier Ltd.
Peer-review under responsibility of the organizing committee of EURODYN 2017.

Keywords: thin-walled beams; warping; free vibration; buckling; localized damage; monitoring; experiments; finite differences code; 1-D model.

1. Introduction

Open thin-walled beams are often used in applications, thus investigations on their behavior are of interest within the scientific community. Several models were proposed to describe their finite and linearized kinematics since the beginning of the 20th century, and analytical and numerical procedures were developed to solve the relevant static and dynamic problems. Some of the authors dealt with one of such models, direct, one-dimensional, and enriched with a coarse warping descriptor [1]; some benchmark cases in free vibration and buckling, of symmetric [1,2] and non-symmetric [3,4] profiles, were investigated analytically, experimentally, and numerically.

* Corresponding author. Tel.: +39-011-090-4873; fax: +39-011-090-4899.
E-mail address: gianfranco.piana@polito.it; gianfranco.piana@uniroma1.it

1877-7058 © 2017 The Authors. Published by Elsevier Ltd.
Peer-review under responsibility of the organizing committee of EURODYN 2017.
10.1016/j.proeng.2017.09.012

In this contribution, the effect of localized cross-section reductions on free dynamics and stability of the non-trivial equilibrium paths of compressed open thin-walled profiles is analyzed. Indeed, it is well known that such reductions may model localized damage in a direct problem, with an outlook to damage monitoring and identification. To this aim, the *in-house* finite differences code proposed in [1] is here enhanced to account for cross-section variations along the beam axis. The new code is tested on the benchmark case of a beam with double I cross-sections, exhibiting non-negligible warping rigidity. The cross-section reduction is operated by removing the flanges on a small part of the beam (about 1% of the total length), thus yielding a cruciform cross-section with negligible warping stiffness. Different end warping constraint conditions are analyzed: free, half-, and fully restrained warping. For all of these cases, the results of the direct model are compared to finite element and/or experimental results.

2. Direct beam model and finite difference code for thin-walled open beams with variable cross-section

The model in [1] is direct, one-dimensional, and describes stretch, shearing, bending, and torsion; an additional scalar parameter coarsely measures the average warping of the cross-section. Finite kinematics yields linearized strain measures; an inner constraint between warping and twist is introduced. The balance of power (or virtual work) gives the balance of force and torque, plus the auxiliary equation for bi-shear and bi-moment. Both conservative and non-conservative loads can be considered. Non-linear hyper-elastic constitutive relations, plus boundary conditions, complete the governing equations. Details on the model can be found in [1] (see Section 2, in particular).

The *in-house* numerical code adopted to investigate the behavior of the beams described by the model sketched above is written in terms of finite differences. It allows to studying non-trivial equilibrium paths (resorting to a non-linear solver), and investigating their stability by standard Ljapounov criteria (imposing a small perturbation to the path, hence obtaining a non-standard eigenvalue problem). However, only uniform beams were considered so far; thus, a refinement is necessary to analyze beams with variable cross-section. The differential governing equations are first-order in space, thus the finite difference scheme is central, and all derivatives (e.g., f') are rewritten as

$$\frac{f_{n+1}-f_n}{\Delta L_n}, \qquad n=1,2,...N$$

while all other unknowns and quantities (e.g., g) are expressed as

$$\frac{g_{n+1}+g_n}{2}, \qquad n=1,2,...N$$

Here, f_n and g_n are the nodal values of the relevant functions, ΔL_n is the distance between adjacent nodes (the length of the interval), and N is the number of intervals. A simple way to insert a variation in the section properties is to refresh the constitutive relations of the elements affected by the variations. Since the governing equations are at most first-order differential in space, a cross-section variation is modeled as a singular element. Thus, the model is unaltered from a theoretical point of view: the only refinement required is related to the numerical implementation.

The main features of this model and of the relevant implementation are: a) the beam model is direct, 1-D, Timoshenko-like, and warping-dependent; b) kinematics is finite, cross-sections are generic and variable, constitutive relations are non-linear; c) conservative and non-conservative loads can be considered; d) non-trivial equilibria are found; e) their stability and possible bifurcations, either static (buckling) and dynamic (flutter), is investigated.

3. Analysis of a benchmark case

A thin-walled profile of aluminum 6060-T5, with cross-section shown in Fig. 1 (parts in red and white together), is chosen as benchmark. The beam length (clear span in the experiments) is 950 mm, and the mechanical properties are: Young's modulus 69 10^9 Nm^{-2}; Poisson's ratio 0.3; mass density 2600 kgm^{-3}. Displacements and rotations are prevented at one end; at the other end the longitudinal displacement is allowed in the numerical simulations, and imposed in the experiments. Such a beam was object of previous investigations of the authors: in particular, the *in-house* code predictions in terms of natural frequencies and buckling loads of the undamaged beam were compared to the analytic solutions (when available) and to the experimental and/or finite element results [2]. Here, by means of

the upgraded version of the *in-house* finite difference code sketched above, we analyze the same beam, with a localized cross-section reduction introduced by removing the flanges on a small portion of the beam (10 mm long, about 1% of the length). This yields a cruciform cross-section with negligible warping stiffness, see Fig. 1 (part highlighted in red). The center of the beam segment with reduced section is placed at one fourth of the axis length.

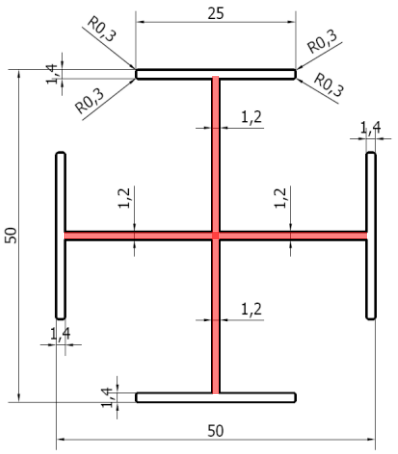

Fig. 1. Cross-section of the beam selected as benchmark (dimensions in mm). The red area shows the reduced cross-section.

3.1. In-house *code results*

The analysis with the *in-house* code requires the values of: beam length l, Young's modulus E, Poisson's ratio ν (whence the shear modulus $G=E/[2(1+\nu)]$), material density ρ, and cross-section area measures. The values for l, E, ν, ρ, were given in the previous section; the cross-section area properties in a central Cartesian system $\{O, x_1, x_2, x_3\}$ are listed in Tab. 1, where: A, A_j are the area and direct shear shape modified areas, respectively; J is the Saint-Venant's torsion factor; I_c is the polar moment of inertia with respect to the shear center; I_j are the central principal moments of inertia; and Γ is the warping constant (i,j = 2,3). Since both the full and reduced cross-sections are doubly symmetric, the shear and bending-torsion coupling terms vanish and the shear center coincides with the center of area. Tab. 1 also shows the percentage reductions in the cross-section properties: all values, especially flexural and warping stiffness, dramatically decrease (the latter is zero for the reduced section).

Tab. 1. Geometrical properties of the full and reduced cross-sections.

Cross-section	A, mm^2	$A_2=A_3$, mm^2	J, mm^4	I_c, mm^4	$I_2=I_3$, mm^4	Γ, mm^6
Full	251.84	110.38	148.36	111,028	55,514	4,305,656
Reduced	111.84	49.81	54.53	21,044	10,522	0
Diff., %	–56%	–55%	–63%	–81%	–81%	–100%

Free, semi-, and fully restrained warping constraints are introduced at the ends of the beam. Semi-restrained warping is considered so to match the experimental condition provided by the end joints, which prevent penetration, but allow detachment. Indeed, a peculiar feature of the code is the simplicity and effectiveness in simulating this special constraint: it is sufficient to run the code under fully restrained warping conditions, with a warping constant equal to half the actual value. Fig. 2 shows the numerical results in terms of fundamental frequencies vs. applied compressive axial loads; the beam is divided into 95 elements of constant length equal to 10 mm, of which only one has reduced sectional properties (10 mm is the length of the modified portion), while the others have the unaltered ones.

Two main conclusions may be drawn. Firstly, the buckling loads, corresponding to vanishing natural frequencies (bold-faced values in Fig. 2) are clearly affected by the local reduction of the cross-section, since the frequency–load curves of the undamaged and damaged specimens are quite distinct near the relevant critical loads. The decrease of the buckling loads is 46%, 14%, and 18%, for free, semi- and fully restrained warping conditions. Secondly, the initial paths (i.e., for low compressive load levels) of the semi- and fully restrained warping conditions are almost overlapped, suggesting that in these cases the inverse problem of damage identification could be very challenging.

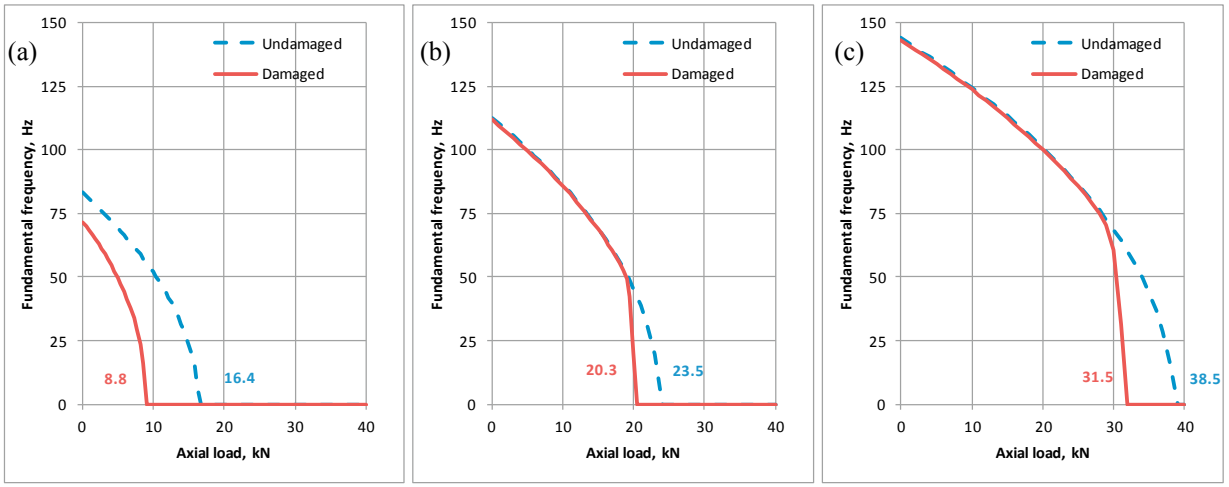

Fig. 2. Numerical fundamental frequency–load paths for: (a) free; (b) semi-restrained; and (c) fully restrained end warping.

3.2. Comparison with finite element and experimental results

The previous numerical results are compared to experimental ones, and to the numerical predictions provided by the commercial finite element code Axis VM 12 [5]. The experimental setup is the same as in [2,6]; the main aspects are summarized hereafter. The specimens were compressed, till buckling, by an MTS universal machine that imposed an axial displacement to a beam end. The natural vibration frequencies were extracted, for different compressive forces, by means of piezoelectric pickups stuck on the beam surface. Such sensors allow for precise frequency identification up to 20-22 kHz [7]. All end rotations and displacements were prevented by suitable constraints. Regarding end warping restraints, two conditions were realized in the lab, i.e., free and partially (semi-) restrained warping (see above). The obtained experimental frequency–load curves can be used for buckling load prediction. Moreover, finite element modal and buckling analyses were run after modeling the beams with shell elements; the two conditions of free and fully restrained warping of the ends of the beam were analyzed.

Fig. 3 shows the experimental vs. numerical (FEM) buckling modes for the two constraint conditions. In both cases, the beam underwent torsion buckling, with the maximum rotation at the weakened section. In Fig. 3a, end warping is completely free for the flanges in both the experimental setup and finite element simulation. In Fig. 3b, end warping is fully restrained in the simulation, whereas in the experiments the detachment of the ends from the joints is not prevented; therefore, the lab constraints closely represent a semi-restrained warping condition. In addition, the cross-section reduction, extended for 10 mm along the beam axis, presents rounded angles (radius = 5 mm) in the experiments, and right angles in the finite element and *in-house* models (see again Fig. 3).

Fig. 4 presents the experimental fundamental frequency–load curves for both the analyzed constraint conditions. These trends are similar to those in Fig. 2, but differ because of the inevitable imperfections present in the real lab realization of the experiments (see [2,6]). Actually, a model updating could improve the match among the plots, but this is not of primary importance in this study. Indeed, the trends can be always used for a preliminary prediction of the buckling load: in fact, the fundamental frequency of an imperfect beam should generally exhibit a minimum near

the critical load [8,9]. Thus, according to this simple criterion, limiting the analysis to the fundamental frequency yields predicted buckling loads equal to about 14.5 and 18 kN for the free (Fig. 4a) and the semi-restrained (Fig. 4b) warping case, respectively. In general, the buckling load prediction based on measured frequency–load curves is not an easy task, and numerical calculations like those of Section 3.1 are, thus, of great help.

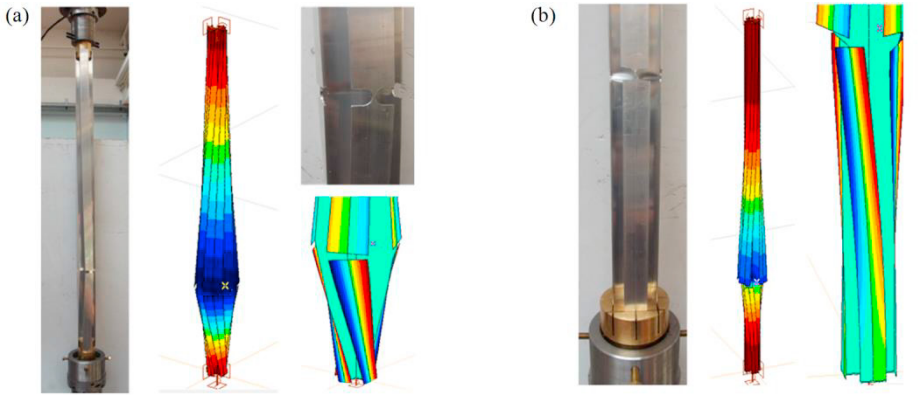

Fig. 3. Experimental vs. numerical (FEM) torsion buckling for: (a) free; and (b) restrained end warping.

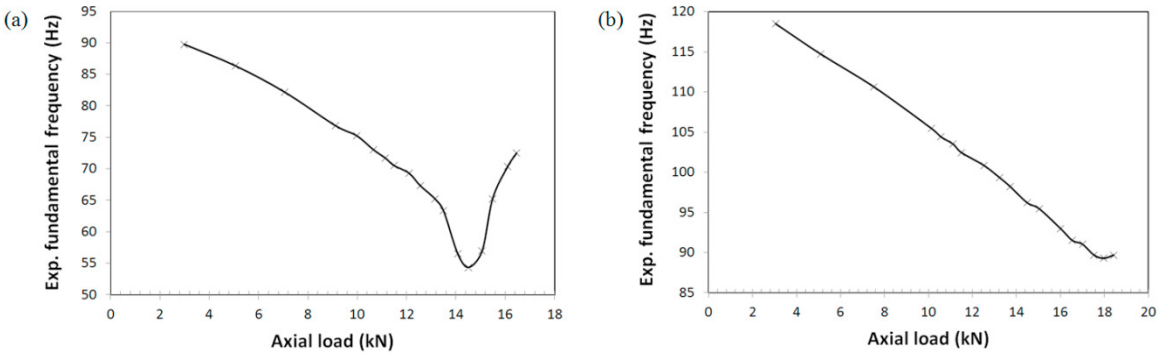

Fig. 4. Experimental fundamental frequency–load paths for: (a) free; and (b) semi-restrained end warping.

A comparison of experimental and numerical results in terms of buckling loads and fundamental frequencies of unloaded beams is proposed in Tab. 2 (where FDM stands for the results obtained by the *in-house* code).

Tab. 2. Experimental vs. numerical critical loads and fundamental frequencies for different constraint conditions.

	N_{cr} Exp. (kN)	N_{cr} FEM (kN)	N_{cr} FDM (kN)	f_1 Exp.[(1)] (Hz)	f_1 FEM[(2)] (Hz)	f_1 FDM[(2)] (Hz)
Free warping	14.5	9.8	8.8	89.7	69.1	71.6
Semi-restrained warping	18.0	–	20.3	118.5	–	111.8
Fully restrained warping	–	29.6	31.5	–	134.0	143.0

[(1)] Beam under a compressive load of 3 kN; [(2)] Unloaded beam.

An analysis of Tab. 2 shows the potentialities of the *in-house* numerical code based on the adopted beam model versus the shell numerical commercial code, as far as these global quantities are concerned. Indeed, it is apparent that 95 intervals can easily and satisfactorily reproduce the same results of some thousands of finite elements. It is apparent that both numerical approaches provide similar results in terms of buckling load and natural frequencies, thus confirming the validity of the approach. On the other hand, the experimental results show the same trend as the

numerical ones, but return a somewhat stiffer behavior with respect to the latter. This is physically reasonable for a series of reasons. Firstly, the actual end constraints realized in laboratory actually provide stiffer conditions with respect to the theoretical ones. In second place, the imposed damage will not, reasonably, completely eliminate the warping stiffness at the damaged element, as we imposed numerically. Third, the technological actuation of the damage inevitably brings local hardening of the material, which obviously is not reported in the numerical models. In addition, the local damaged section acts as a local constraint between two adjacent regular chunks of beam, while we modelled it as a regular chunk with different mechanical properties for simplicity of numerics. An updating will surely improve the reliability of the results; further investigations are in due course.

4. Final remarks

A numerical *in-house* code for investigating free dynamics and stability of non-trivial equilibrium configurations of open thin-walled beams with weakened cross-section has been proposed. The code is based on a central version of the finite differences technique, and refines a previous version proposed by some of the authors for the investigation of free dynamics and stability of prismatic beams. The field equations are obtained by a direct and geometrically exact one-dimensional model, in which warping is provided through a coarse scalar descriptor. An updating of the cross-section properties properly describes the weakening of the cross-sections, which affects the global behavior, without changing the main sketch of the code. This allows to considering both sharp (e.g., fatigue cracks) and broad (e.g., tapered beams) variations.

As a meaningful application, the effect of a local cross-section weakening was analyzed here. Adopting a beam with double I cross-sections, exhibiting non-negligible warping rigidity, the weakening is introduced by removing the flanges on a small portion of the beam. Such a reduction simulates a local damage, strongly affecting the beam bending and torsion rigidities. Comparisons among the results provided by the proposed code and the ones furnished by finite element and/or experimental simulations confirm the validity of the proposed technique. On the other hand, this study provides a quantitative measure of the effect of a warping stiffness reduction on the global critical loads, which is an important issue in structural design.

Acknowledgements

The Authors gratefully acknowledge the support of institutional grants of the University “La Sapienza”, Rome, Italy, and of National grant PRIN 2015TTJN95, “Identification and monitoring of complex structural systems”.

References

[1] E. Lofrano, A. Paolone, G. Ruta, A numerical approach for the stability analysis of open thin-walled beams, Mech Res Commun 48 (2013) 76–86.
[2] G. Piana, E. Lofrano, A. Manuello, G. Ruta, A. Carpinteri, Compressive buckling for symmetric TWB with non-zero warping stiffness, Eng Struct 135 (2017) 246–258.
[3] M. Brunetti, E. Lofrano, A. Paolone, G. Ruta, Warping and Ljapounov stability of non-trivial equilibria of non-symmetric open thin-walled beams, Thin Wall Struct 86 (2015) 73–82.
[4] G. Piana, E. Lofrano, A. Manuello, G. Ruta, Natural frequencies and buckling of compressed non-symmetric thin-walled beams, Thin Wall Struct 111 (2017) 189–196.
[5] www.axisvm.eu
[6] G. Piana, A. Carpinteri, E. Lofrano, R. Malvano, A. Manuello, G. Ruta, Experimental and Numerical Elastodynamic Analysis of Compressed Open Thin-walled Beams, in: M. Mains (Ed.), Topics in Modal Analysis & Testing, Volume 10: Proceedings of the 34th IMAC, A Conference and Exposition on Structural Dynamics, Conference Proceedings of the Society for Experimental Mechanics Series, Springer, 2016, pp. 125–138.
[7] G. Piana, E. Lofrano, A. CArpinteri, A. Paolone, G. Ruta, Experimental modal analysis of straight and curved slender beams by piezoelectric transducers, Meccanica 51 (2016) 2797–2811.
[8] A. Carpinteri, R. Malvano, A. Manuello, G. Piana, Fundamental frequency evolution in slender beams subjected to imposed axial displacements, J Sound Vib 333 (2014) 2390–2403.
[9] L.N. Virgin, Vibration of axially loaded structures, Cambridge University Press, New York, 2007.